

Hydrological projections of climate change scenarios over the 3H region of China: A VIC model assessment

Li Dan,¹ Jinjun Ji,¹ Zhenghui Xie,² Feng Chen,² Gang Wen,³ and Jeffrey E. Richey⁴

Received 7 November 2011; revised 18 April 2012; accepted 18 April 2012; published 1 June 2012.

[1] To examine the potential sensitivity of the Huang-Huai-Hai Plain (3H) region of China to potential changes in future precipitation and temperature, a hydrological evaluation using the VIC hydrological model under different climate scenarios was carried out. The broader perspective is providing a scientific background for the adaptation in water resource management and rural development to climate change. Twelve climate scenarios were designed to account for possible variations in the future with respect to the baseline of historic climate patterns. Results from the six representative types of climate scenarios (+2°C and +5°C warming, and 0%, +15%, -15% change in precipitation) show that rising temperatures for normal precipitation and for wet scenarios (+15% precipitation) yield greater increased evapotranspiration in the south than in the north, which is confirmed by the remaining six scenarios described below. For a 15% change in precipitation, the largest increase or decrease of evapotranspiration occurs between 33 and 36°N and west of 118°E, a region where evapotranspiration is sensitive to precipitation variation and is affected by the amount of water available for evaporation. Rising temperatures can lead to a south-to-north decreasing gradient of surface runoff. The six scenarios yield a large variation of runoff in the southern end of the 3H, which means that this zone is sensitive to climate change through surface runoff change. The Jiangsu province in the southeastern part of the 3H region shows an obvious sensitivity in soil moisture to climate change. On a regional mean scale, the hydrological change induced by the increasing precipitation from 15% to 30% is more obvious than that induced by greater warming of +5°C relative to +2°C. These simulations identify key regions of sensitivity in hydrological variation to climate change in the provinces of 3H, which can be used as guides in implementing adaptation.

Citation: Dan, L., J. Ji, Z. Xie, F. Chen, G. Wen, and J. E. Richey (2012), Hydrological projections of climate change scenarios over the 3H region of China: A VIC model assessment, *J. Geophys. Res.*, 117, D11102, doi:10.1029/2011JD017131.

1. Introduction

[2] China's water resources per capita rank in the bottom 25 of all countries globally [Song *et al.*, 2005]. The Huang-Huai-Hai Plain region (3H) of northeastern China (Figure 1), with a population of 425 million people, including the megacity of Beijing, produces 50% of China's grain, and

houses 35% of its industry. Water resources per capita in the 3H are only one-third of the country's average level [Wu and Xu, 1997], and only one-half of the standard set by the United Nations to meet socio-economic development [Zhou and Zhang, 2004]. As a result, the water demand in the 3H is large, and continuously increasing, with available water resources completely allocated.

[3] Crops in the 3H are heavily dependent on irrigation from runoff and groundwater [Chinese Academy of Sciences, 2007]. Runoff is also an important source of water harvesting, not only for irrigation but for drinking water, especially north of 35°N in northern 3H [Xu, 1995]. Surface water stores (dams, reservoirs, lakes, wetlands) filled by runoff are important for water supply in the region (including the Miyun Reservoir, the primary source of drinking water for Beijing). Available surface water has to be supplemented by groundwater extraction, at a constantly increasing rate [Xia *et al.*, 2008]. The current natural recharge rate of groundwater, 70% of which comes from precipitation, is 6.3×10^{10} m³/year across the 3H [Ying, 2006], with regulated recharge in northern China [Cai, 2008]. Current real groundwater extraction in the 3H is 6.1×10^{10}

¹START Temperate East Asia Regional Center and Key Laboratory of Regional Climate-Environment for Temperate East Asia, Institute of Atmospheric Physics, Chinese Academy of Sciences, Beijing, China.

²LASG, Institute of Atmospheric Physics, Chinese Academy of Sciences, Beijing, China.

³Policy and Program Department, China CDM Fund Management Center, Ministry of Finance, Beijing, China.

⁴School of Oceanography, University of Washington, Seattle, Washington, USA.

Corresponding author: L. Dan, Key Laboratory of Regional Climate-Environment for Temperate East Asia, Institute of Atmospheric Physics, Chinese Academy of Sciences, Beijing 100029, China. (danli@tea.ac.cn)

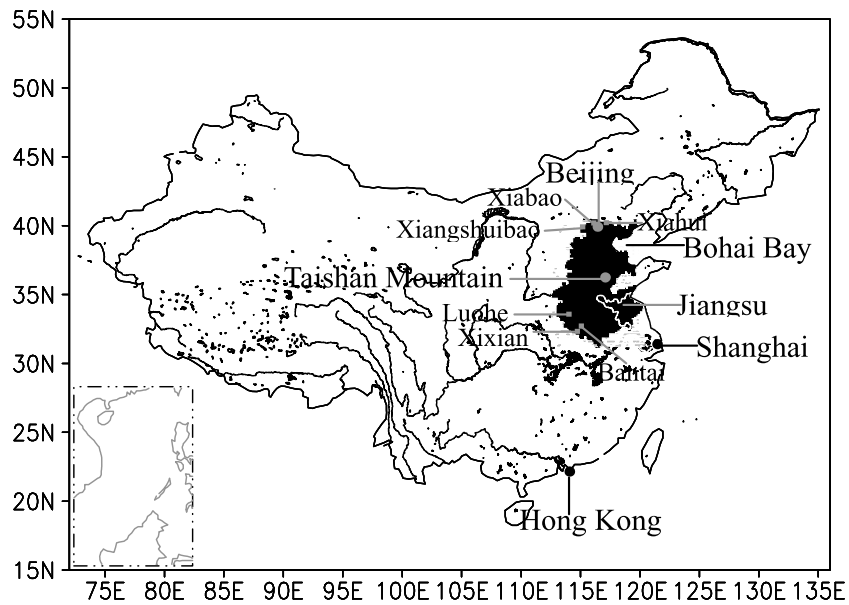


Figure 1. The geographical location of Huang-Huai-Hai (3H) plain in China. (The shaded area means 3H. The inset at the bottom left corner is the South China Sea border.)

m^3/year across the region, relative to the available extraction of $4.7 \times 10^{10} \text{ m}^3/\text{year}$. Over extraction is occurring in some cities and provinces; e.g., 159% for Beijing and 106% for Hebei province.

[4] If the availability of water resources is further reduced by climate change, coupled with increasing demands by industrial, urban and rural domestic use, the long-term capacity for grain production in the region will be seriously affected, potentially threatening China's overall food security. The most robust response is to develop adaptation strategies, based on the best possible knowledge of how water distributions might evolve, and how to optimize water utilization for agriculture and other uses. The current lack of such an integrated analysis is a tremendous handicap when proposing and designing effective climate change adaptation strategies and actions. Hence there is an urgent need to explore possible future changes of surface water resources in order to build a firm scientific basis for adaptation.

[5] The question being addressed in this paper is, how sensitive are the water resources distributed across the 3H to potential changes in precipitation and temperature induced by climate change? Wang *et al.* [2011] used a macroscale hydrologic model (VIC, Variable Infiltration Capacity) with climate scenarios generated by the Hadley Centre RCM system-PRECIS regional climate model to analyze annual runoff scenarios across China, at a 50 km resolution. They concluded that the pattern of "north dry and south wet" would probably be exacerbated, and that regional water shortages and regional flooding remain the key issues that are likely to grow in importance. But more specific, regional effects are not known. We report here on the hydrologic distributions that would be expected across the 3H region from possible variations in future climates with respect to the baseline of historic climate changes. We use the VIC hydrological model, applied a 10 km resolution, to examine how the results of 12 climate scenarios would produce patterns in precipitation, ET, runoff, and soil moisture. This

resolution is necessary to see the more detailed regional patterns relevant to adaptation strategies.

[6] This is the first project on climate adaptation in the 3H region, and forms part of the scientific basis for the adaptation to climate change component of the "Mainstream Adaptation to Climate Change into Water Management and Rural Development" (MACC) project, developed by the State Office of Comprehensive Agriculture Development (SOCAD) of the Ministry of Finance (MOF) in China and the World Bank (WB), and financed by the Special Climate Change Fund (SCCF), under the management of the Global Environment Facility (GEF).

2. Study Region, Data, and Model Description

2.1. The 3H Plain

[7] The Huang-Huai-Hai Plain (3H) of northern China incorporates five provinces (Jiangsu, Anhui, Shandong, Henan and Hebei) and two municipalities of Beijing and Tianjin (Figure 1). The area encompasses about $387,000 \text{ km}^2$, extending from 113°E to the eastern coastline, and from 32°N to 40.5°N [Gong, 1985]. This region has a monsoon climate, with an annual amount of sunshine of 2100–2900 h. The annual precipitation varies from 500 mm to 800 mm, but 60–80% of precipitation occurs in the summer (June to September), in the form of rainstorms or heavy rain. The multiyear mean annual potential evapotranspiration (ET) is about 1100 mm [Liu *et al.*, 2010].

[8] The 3H region is one of the nine principal agricultural zones in China, with a crop production feeding about 32% of the Chinese people, providing about 69% of the wheat and 35% of the maize yield of China. The primary cropping cycle is rotating systems of winter wheat and summer maize, with double cropping as the common planting method across the 3H [Mo *et al.*, 2006]. The double cropping cycles were implemented in response to hydrological change [Liu *et al.*, 2010]. Cropping cycles also include winter wheat-summer

Table 1. Temperature and Precipitation Variation in the 3H Region Under Climate Scenarios of Global Models From IPCC3^a

Region	Temperature Variation (°C)				Precipitation Variation (%)			
	2020s	2050s	2070s	2100s	2020s	2050s	2070s	2100s
Yellow River								
A2	1.3	2.8	4.7	5.9	-1	4	9	12
B2	1.5	2.7	3.7	4.1	0	5	8	11
Hai River								
A2	1.4	2.9	4.7	6.0	0	0	7	17
B2	1.5	2.7	3.8	4.1	2	4	7	17
Huai River								
A2	1.2	2.6	4.2	5.4	0	2	11	16
B2	1.3	2.4	3.5	3.8	1	2	5	11

^a*Qin et al.* [2005].

maize, winter wheat-summer soy, winter wheat-cotton, winter wheat-summer peanuts, and winter wheat-rice [*Chinese Academy of Sciences*, 2007].

[9] From spring to early summer, wheat yield is affected by the lack of precipitation. During summer, too much runoff and too little infiltration from heavy rain is detrimental to maize production. Variation of rainfall over 3H causes drought in the spring and flood in the summer. Consequently, natural water resources are not sufficient to support agricultural production. Crops need irrigation in drought conditions, which, with declining precipitation, has recently made groundwater extraction a serious problem [*Chinese Academy of Sciences*, 2007].

2.2. The VIC Model Description

[10] The VIC model is a large-scale, semi-distributed land hydrological model developed in conjunction between the University of Washington and Princeton University [*Liang et al.*, 1994]. It computes the budgets of surface energy and water, taking into account saturation, excess runoff and infiltration, snow melting, and soil freeze-thaw processes [*Liang et al.*, 1996; *Cherkauer et al.*, 2003; *Nijssen et al.*, 2001a; *Elsner et al.*, 2010]. VIC can be applied to multiple spatial scales and can be temporally discretized to be hourly, daily, monthly and yearly time scales. Vegetation is described by the leaf area index (LAI), canopy resistance, and the relative proportion of roots in soil. For the three soil layers, the top layer (layer 1) is thin, at 10 cm, and can quickly respond to rainfall by evapotranspiration. The upper soil layer regulates infiltration and excess runoff, and controls the quick flow component. The third layer controls base flow generation.

2.3. Data Sources

[11] For the historic climate change analysis, meteorological data (including maximum and minimum daily temperature and daily rainfall) were taken from observation data of meteorological observation stations across all of China. The data set, the *740 Stations Meteorological Data*, was released by the China Meteorological Administration, with strict quality control over the 3H. The temporal range of the daily data spans from 1980 to 2000. For the high resolution application here, the data was spatially homogenized and processed into grid cells of 10 × 10 km [*Xie et al.*, 2004], with a temporal resolution of 1 day. VIC was driven by the meteorological data to simulate the surface hydrology of 4286 grid points in the 3H region.

[12] The soil and vegetation parameters were derived using the *Food and Agriculture Organization* [1998] and the University of Maryland land cover data, as in *Nijssen et al.* [2001c] and *Su et al.* [2008]. The land cover data (11 vegetation types, with open water bodies and urban area treated as bare ground) were upscaled from the 1 km data set to the 10 km model grid, by calculating the summed proportion of each vegetation type in the 10 km grid cell, and aggregating the final value from the weighted average in the cell. The leaf area index (LAI) data was prescribed with monthly data from the Land Data Assimilation System developed by the National Aeronautics and Space Administration (<http://ldas.gsfc.nasa.gov/>). This prescribed phenology and VIC model structure does not allow temperature sensitivity experiments, nor does it a priori represent the actual phenology that might result under conditions of increased temperature. Rather, results should be interpreted as changes given a fixed phenology. Soil parameters were derived from the global 5-min data provided by NOAA hydrological office [*Xie et al.*, 2007].

2.4. Climate Scenarios and Downscaling

[13] The A2 (a world of moderately fast economic growth and only modest reduction in fossil fuels) and B2 (a world of more modest economic growth and less dependency on fossil fuels) scenarios adopted by the International Panel on Climate Change (IPCC) assessment are used as the basis for our 12 climate scenarios. Results for the two scenarios (A2 and B2) were taken as multimodel averages from more than 40 global models [*Qin et al.*, 2005]. Under these two scenarios, temperature would increase by about 2°C in the 3H by 2020–2050 and by 5°C by 2100. Precipitation would increase 0–5% in 20–30 years and 10–20% in 100 years (Table 1).

[14] Future climate scenario results must be downscaled, for the hydrologic simulations. The choice of the downscaling method is influenced by the necessary spatiotemporal resolution, resources required, and physical consistency. A rapid impact assessment based on “change factors” (CFs) [*Arnell*, 2003; *Diaz-Nieto and Wilby*, 2005] was used here. CFs scenarios are recommended to use for broad, high-level assessment and identification of vulnerable regions [*Diaz-Nieto and Wilby*, 2005], such as this 3H assessment. The method is computationally straightforward and quick to apply for future hydrological calculations. The scenarios were derived by simply adding the temperature change projected by the models (+2°C and +5°) and the precipitation change (±15% and ±30%) to the daily baseline time series (e.g., in scenarios with 2°C increase, a value of 6°C will become 8°C by adding 2°C).

[15] This simplified downscaling method is quite similar to the change factor (CF) method used by other hydrological simulations, [e.g., *Minville et al.*, 2008; *Prudhomme et al.*, 2010]. This CF method together with other relatively simple downscaling approaches; e.g., the delta approach [*Elsner et al.*, 2010] and pattern-scaling approach [*Todd et al.*, 2010; *Arnell*, 2011], can be classified as “empirical downscaling methods,” which are not resource intensive [*Winkler et al.*, 2011]. The CF and delta approach both use monthly variables from climate models to modify the historic daily time series needed for hydrological modeling [*Hamlet and Lettenmaier*, 1999; *Minville et al.*, 2008]. The delta method has been discussed in detail by *Kirono et al.* [2011].

[16] The pattern-scaling method only works at the monthly scale [Todd *et al.*, 2010], and assumes the linear linkage of climate variables with the global mean temperature, which may not be appropriate at high temperature change [Todd *et al.*, 2010; Arnell, 2011]; e.g., the 5°C change of this simulation. The pattern-scaling approach cannot show the relative change of different precipitation intensity, which may underestimate the potential hydrological change [Arnell, 2011]. The CF approach cannot change the wet days and the spatial variability [Minville *et al.*, 2008; Diaz-Nieto and Wilby, 2005], thus this hydrological projection of 3H may depart partly from the actual change in the future. But the north-south gradient change will not be altered according to the absolute change of climate variables and topography of 3H. As a consequence of these limitations, we focus on the variations in the amplitude of future surface hydrological changes, rather than as potential changes in precipitation structure.

2.5. Model Calibration and Validation

[17] The hydrological data from six basins in the 3H were used for model calibration and validation [Xie *et al.*, 2007]. Three basins (Xiahui, Xiabao and Xiangshuibao) are located in Hai River Basin of far northern 3H, with an annual mean precipitation of 400–500 mm and 75–85% of the rainfall occurring in the flooding season. There is tremendous conflict in the water supply and demand in the Hai River basin, with extensive anthropogenic water withdrawal from river channels and groundwater for agricultural and industrial production. Three basins (Luohe, Xixian and Bantai) are located in the Huai River basin of southwestern 3H (Figure 1), with an annual mean temperature of about 11°–16°C and an annual mean precipitation of 700–1300 mm. Rainfall in the Huai River basin is variable, where the maximum annual precipitation can be 3–4 times the minimum.

[18] Streamflow data from the Chinese Ministry of Water Resources [Xie *et al.*, 2007] was used to calibrate VIC model parameters, by comparing the simulated daily runoff, which was routed to the outlets of the river basins, to the observed streamflows of those basins (Figure 2). Then the calibrated model was used again for surface hydrological simulations. The calibration or validation period of available data is January 1980 to December 1990 for five basins and January 1980 to December 1985 for the Xiabao basin. The data used for calibration represent naturalized flow, as there were no extractions, diversions, and dams during the 1980 to 1990 calibration period.

[19] The main calibration parameters are the thickness of the three soil layers (0.05 to 0.5 m for d_1 , 0.3 to 2.4 m for d_2 , and 1.8 to 2.7 m for d_3), three base flow parameters (Dm, Ds, Ws) of a conceptual base flow model, ARNO, and infiltration parameter b typically ranging from 0 to 0.4. The parameter b defines the shape of the Variable Infiltration Capacity curve, describes the amount of available infiltration capacity as a function of the relative saturated grid cell area, controls the quantity of runoff generation directly and the water balance. A higher value of b gives lower infiltration and yields higher surface runoff. In the calibration process, the basins were grouped by climate and large river basin zones, and the parameters of all basins within the same

climate and large river basin zone were assumed to have the same values [Xie *et al.*, 2007].

[20] The integration with the default parameters of VIC were taken as non-calibrated runs. The calibrated soil depths (d_1 , d_2 , d_3) were commonly set deeper in arid and semiarid regions and lower in humid regions. The Dm, Ds, and Ws parameters were calibrated to fit the low flow, with the infiltration parameter b adjusted to match the observed flow peaks as the calibration parameters for the simulations of the calibrated runs. The monthly mean simulated streamflow was generally improved by calibration, especially for the northern three basins, where the relative root-mean squared error (RRMSE) before and after the calibration was 94.7%/14.3%, 79.5%/7.7%, 162.6%/14.2% for the Xiahui, Xiabao and Xiangshuibao basins, respectively. The RRMSE was 11.8%/10.1%, 11%/9% and 8.8%/7.9% for the southern three basins (Bantai, Xixian and Luohe). For the region without observation data (the adjacent Huang River Basin), the calibrated parameters were transferred from the region with data available based on the climate zones and large river basins [Nijssen *et al.*, 2001b; Xie *et al.*, 2007]. The parameters were then verified by comparing data in the same climate zone and larger river basin, which can be regarded as recalibration. The parameters of the Xiangshuibao are the averages of parameters calibrated at Xiahui and Xiabao, as the three basins belong to the larger basin of Hai River basin. The parameters of the Luohe are the averages of parameters calibrated at Bantai and Xixian, as the three basins belong to the larger basin of Huai River basin. The results of Xiangshuibao (Figure 2c) and Luohe (Figure 2f) are good examples of improvement in simulated streamflow after parameter transfer by recalibration, in contrast with non-calibrated runs.

3. Results and Analysis

[21] Results of the analysis of trends in climate and hydrologic responses from historical conditions to alternative scenarios for the future show a very dynamic system. We first consider trends in climate, where there has been a progressive warming and aridification since the 1950s. Against this backdrop, hydrologic projections under 12 scenarios for climate change are analyzed, where temperature change is used as the background for variation in precipitation. The spatial changes in ET, soil moisture, and runoff across the region, with first a 2°C increase, and then a 5°C increase, relative to the 1980–2000 climate mean, are analyzed. Then, changes in precipitation, ET, runoff, and soil moisture are averaged across the 3H region.

3.1. Climatic Trends

[22] Hydrological projections over China's 3H region were carried out relative to the background of climate change. With global warming, temperature variation over the past 100 years in China has been similar to the rising trend in the Northern Hemisphere [Ding and Dai, 1994]. The warming magnitude in northern China has been more obvious than in southern China. Aridification in northern China has been significant, especially in the 3H river basins, where annual precipitation has decreased by 50–120 mm during the 1956–2000 period [Ren *et al.*, 2005]. Summer precipitation, which is a large share (about 60%) of total annual precipitation, has also been dramatically reduced. Due to the decreasing rainfall, the climate

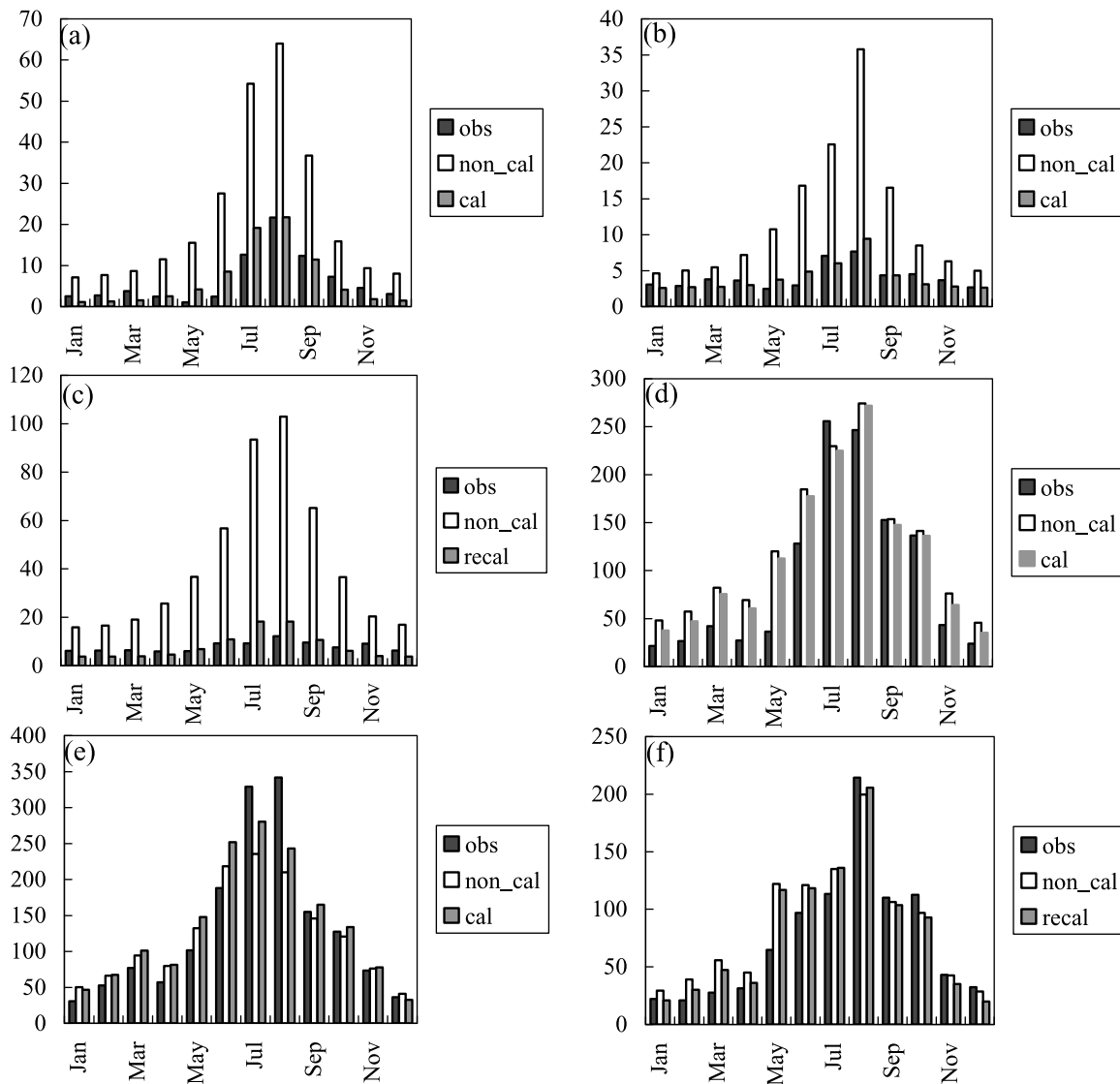


Figure 2. Monthly mean streamflow of 6 basins in 3H: (a) Xiahui, (b) Xiabao, (c) Xiangshuibao, (d) Bantai, (e) Xixian, and (f) Luohe (units: m^3/s). (The symbol obs means observation, non_cal for non-calibration, cal for calibration, recal for recalibration.)

in the 3H region has become drier, while higher temperatures have led to increased soil evaporation. Moreover, these factors combined with human activities of overusing water have resulted in a significant reduction in the recharge of local groundwater resources. A systematic analysis based on hydrological projections will be helpful in understanding the baseline and possible future changes of water resources in the 3H region in China.

[23] The observed change of precipitation is shown (Figure 3) as an anomaly percentage from 1980 to 2000, calculated by: $P_a = \frac{P - P_{\text{clim}}}{P_{\text{clim}}} \times 100\%$, where P is precipitation, and the subscript *clim* represents the climatological state of precipitation averaged during 1980–2000 [Dan et al., 2005]. The anomaly varied between ± 15 –30% in the past 20 years, showing large precipitation variability across the 3H.

[24] To study the surface hydrology baseline, the multiyear annual mean of the four hydrological variables (precipitation,

ET, runoff and soil moisture) were examined with the VIC model (Figure 4). The surface hydrological distribution shows an increasing gradient from north to south, with an obvious boundary around 34°N , especially for ET (Figure 4b). The observed precipitation is below 1.5 mm/day in the north and increases to above 3 mm/day in the southern part of the 3H region. The highest precipitation, centered at 117°E and 36.2°N , is located near the Taishan Mountain area (Figure 1) in the Shandong province. The maximum ET in the southern part of the 3H region reaches up to 1.8 mm/day and the maximum runoff is 1.2 mm/day. The distribution of surface soil moisture (Figure 4d) ranges from 0.09 to $0.39 \text{ m}^3/\text{m}^3$ over the whole region.

3.2. Hydrological Projections Under Climate Scenarios

[25] The possible magnitudes of temperature increase in the 3H under A2 and B2 scenarios were used as the large-scale background in the VIC model. Twelve possible

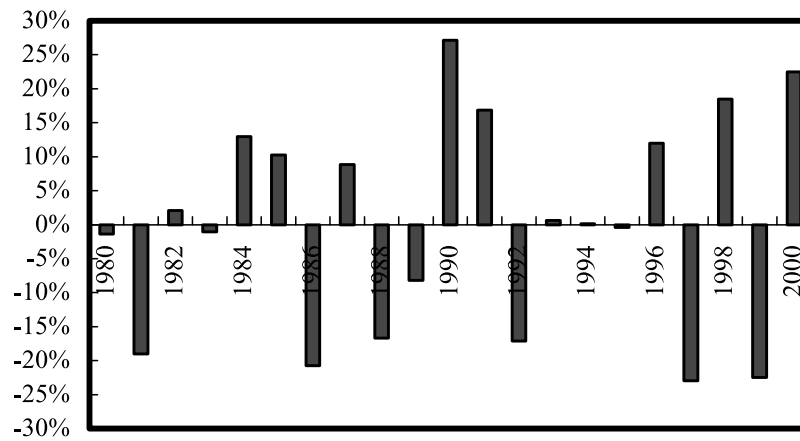


Figure 3. The observed precipitation anomaly percentage relative to the value averaged in the year of 1980–2000. (Values are area-averaged precipitation over the 3H region.)

scenarios of climate change were evaluated, with assumptions of precipitation increasing or decreasing by 15% and 30%, and temperature increasing by 2°C and 5°C, relative to historical conditions (Table 2). The variety among the 12 types of climate scenarios provides sufficient diversity to account for the uncertainty and variation of climate change projections in the 3H region by considering the largest possible variation thresholds of climate. As the focus of this study is on the potential level of change in surface hydrology in response to specific climatological conditions, results are presented only for these conditions, and not for specific future time periods. The results with 30% change of precipitation are similar to the experiments of 15% variation in spatiotemporal patterns, differing only in simulated magnitude. Hence, results for the surface water distributions will be presented only for the 15% change of precipitation in the 12 chosen scenarios, and not for the 30%. Results for the 30% change will be presented later for basin averaged analysis.

3.2.1. Simulations With a 2° Temperature Increase

[26] The result of the surface water change with 2°C warming and 0% change of precipitation in the 3H, minus the climatic mean during 1980–2000 (climate scenario 5, Table 2), shows the unique impact of warming on surface water change excluding precipitation (Figure 5). The ET difference relative to the historic baseline shows the overall increase in the 3H region ranging from 0.01 to 0.08 mm/day, with the increasing ET occurring mainly to the south of 34°N. However, runoff shows the decreasing pattern over the whole 3H region, with the largest decreasing value of up to 0.016 mm/day occurring in the southern part of the region. The top-layer soil moisture shows a slight increase north of 34°N, and an obvious decrease in the Jiangsu province due to the water balance under increasing ET with nearly unchanging amounts of runoff. The slight increase of soil moisture north of 34°N is mainly attributed to snow melting. Increasing temperatures induce more snow to melt, contributing to the slight enhanced soil moisture, although the precipitation does not change (figures not shown). The sublimation difference of snowpack is slightly decreased (less than -0.006 mm/day). This scenario demonstrates that temperature rise over the 3H region will lead to enhanced ET and decreased runoff. The largest change occurs in the southern part of the 3H region for both

variables. The soil moisture of Jiangsu is, therefore, sensitive to climate warming.

[27] The scenario of adding a 15% increase in precipitation to the 2°C temperature rise (scenario 6) makes more surface water available (Figure 6). Precipitation increases more than 0.3 mm/day south of 35°N, but the increment in the north is smaller, below 0.3 mm/day (Figure 6a). Similar to the precipitation change, ET, runoff and soil moisture also show larger changes south of 35°N. Due to the temperature rise and precipitation increase, ET shows an increase ranging from 0.07 to 0.18 mm/day. The largest enhanced region is located in the southwestern part of the 3H, between 33 and 36°N. Compared to the ET of scenario 5 (Figure 5b), the precipitation increase makes more surface water available to evaporate under temperature rise, and hence induces an enhancement of ET north of 34°N, which shows the dominating effect of precipitation in this region. Runoff (Figure 6c) and soil moisture (Figure 6d) increase over the 3H, demonstrating that the enhanced effect of precipitation can exceed the decreasing impact on runoff and soil moisture resulting from temperature rise alone. The runoff increases in the southern part of the 3H, with an increment up to 0.24 mm/day. The soil moisture increases in the north rather than the south and the boundary lies near 34°N. The most obvious enhanced regions are located in the Jiangsu province and Bohai Bay (eastern 3H in 37–40°N).

[28] Under climate scenario 7, with 2°C temperature rise and 15% precipitation decrease, the surface water change shows a general decrease over the entire 3H region (Figure 7). Precipitation (Figure 7a) shows a decreasing gradient from south to north with a decreasing value below -0.2 mm/day (-15%). ET (Figure 7b) generally decreases across the 3H region, with the largest area located in the southwestern part of the 3H region, between 33 and 36°N. However, in the southern end of the 3H region, ET shows a slight increase, which can be attributed to the effect of temperature rise with adequate surface water. The southern part of the 3H region has relatively plentiful amounts of water available for surface evaporation (cf. Figure 4a), so the 15% decrease of precipitation cannot change the increasing pattern of ET. The runoff (Figure 7c) shows a considerable decrease south of 34°N, with a value below -0.1 mm/day (-21%), due mainly to the lower soil moisture content

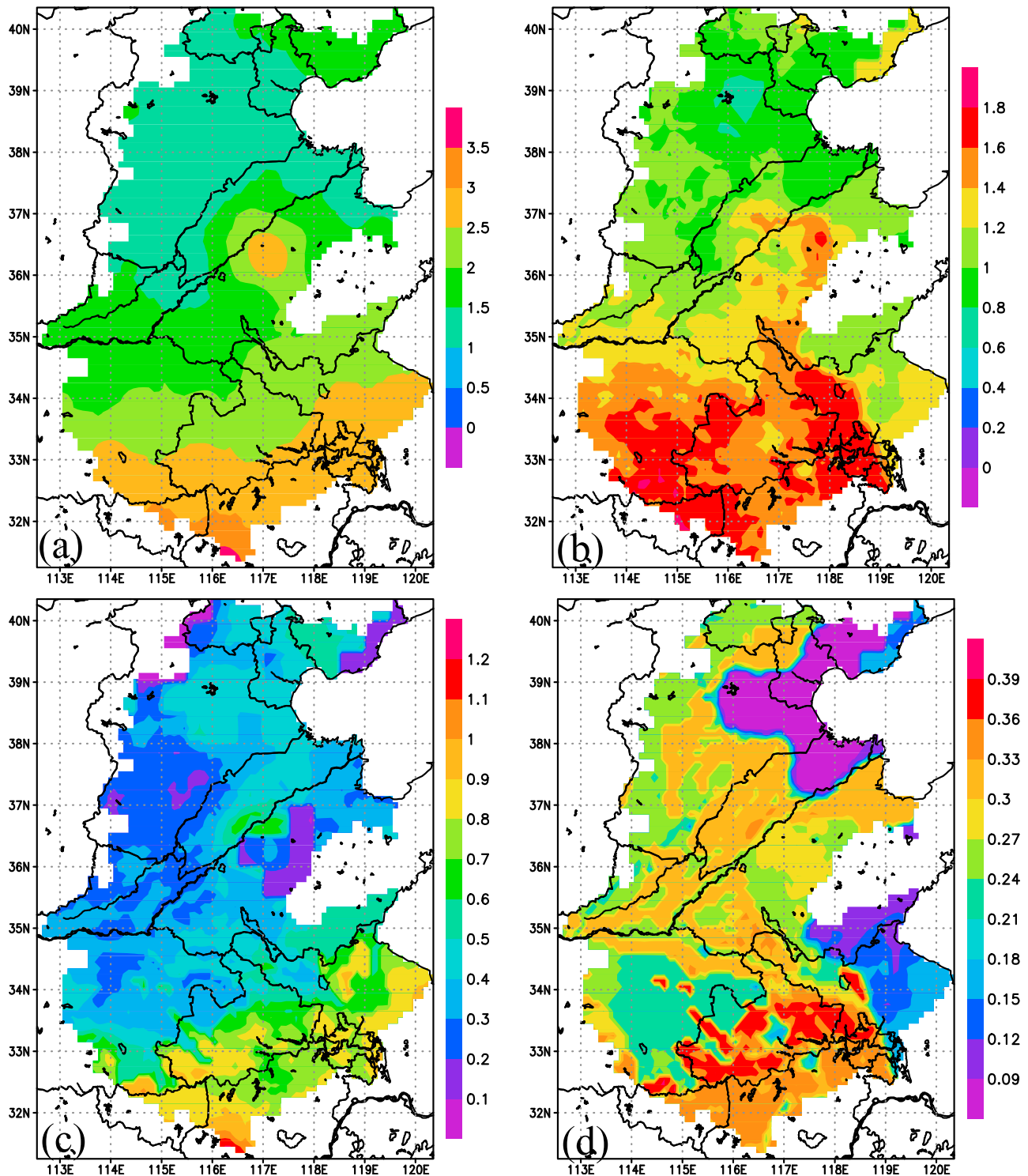


Figure 4. The annual mean surface hydrology averaged in 1980–2000 of 3H over China: (a) the observed precipitation, (b) evapotranspiration (ET), (c) runoff (units: mm/day), and (d) volumetric soil moisture of the top layer (units: m^3/m^3).

resulting in reduced saturation and infiltration excess runoff generation. The variation in the distribution of runoff is similar to the spatial pattern of precipitation change. There is slightly more soil moisture change in the south than in the north, with the most obvious variation still occurring in the Jiangsu province and Bohai Bay.

3.2.2. Simulations With a 5° Temperature Increase

[29] To compare the impact of different temperature changes across the 3H region, climate scenarios 10–12 adopted a 5°C temperature increase. Surface water changes with 5°C warming and zero percentage change of precipitation shows a marked drying (Figure 8). ET (Figure 8b) increases markedly

Table 2. Climate Change Scenarios, Snr, Used for the Water Resource Projection of 3H in VIC

	Normal	+15%	-15%	30%	-30%
Normal	Snr0	Snr1	Snr2	Snr3	Snr4
+2°C	Snr5	Snr6	Snr7	Snr8	Snr9
+5°C	Snr10	Snr11	Snr12	N/A	N/A

to the south of 34°N with a notable increase centered near Taishan Mountain in the central eastern part of the 3H region. This demonstrates that the warming impact on the surface ET mainly occurs in the southern part of the 3H region. Compared to the ET change under 2°C warming (Figure 5b), the spatial pattern is similar, but the magnitude more than doubles over the entire 3H. Runoff (Figure 8c) shows a marked decrease to the south of 34°N with a maximum of -0.045 mm/day. This reduction is approximately three times greater than predicted from the 2°C warming scenario (Figure 5c), especially to the south of 33°N. The runoff

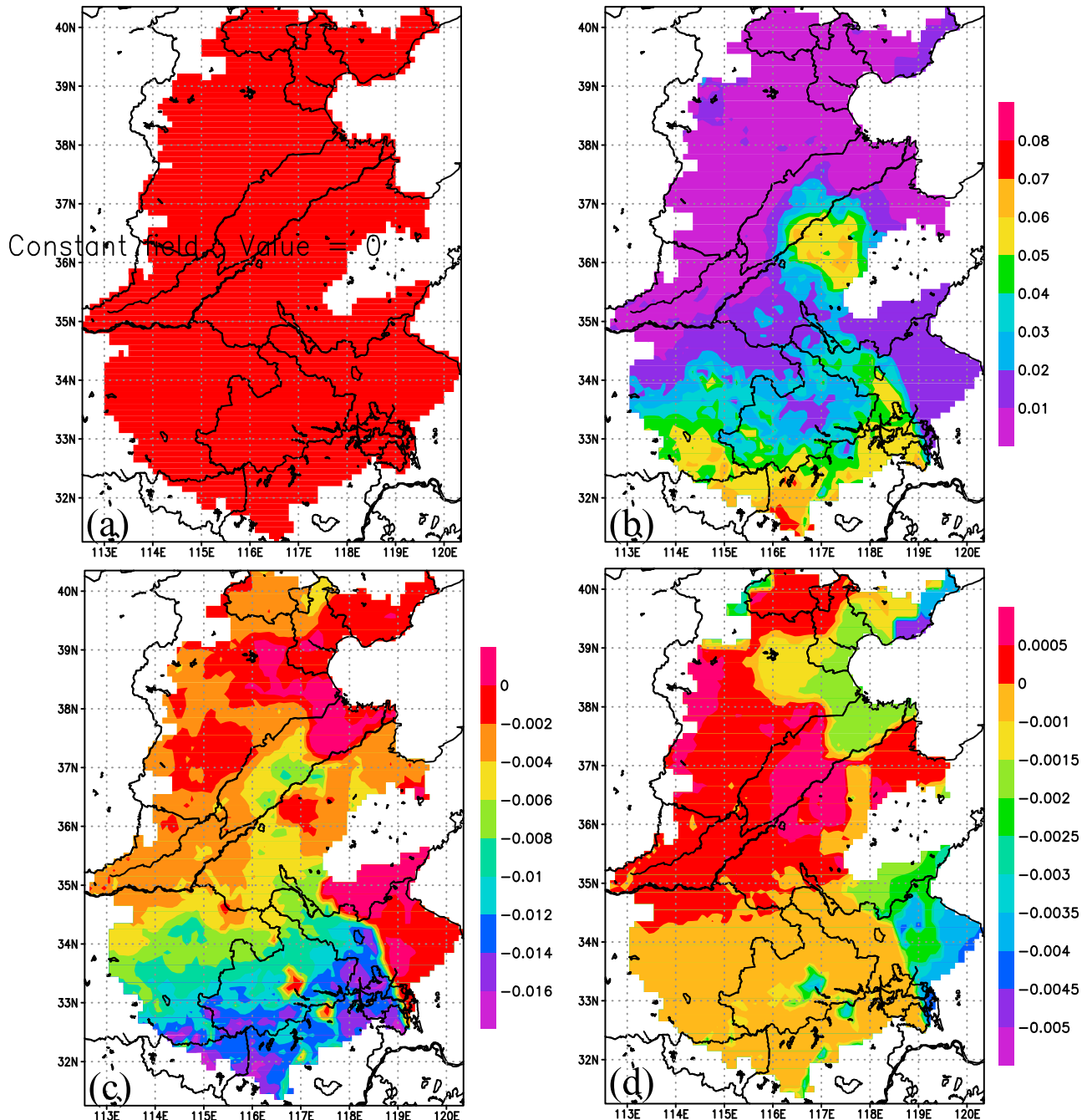


Figure 5. The climatology of the climate scenario 5 (+2°C) minus the normal observed climatology of 3H over China: (a) the precipitation difference, (b) ET difference, (c) runoff difference (units: mm/day), and (d) volumetric soil moisture difference of the top layer (units: m^3/m^3).

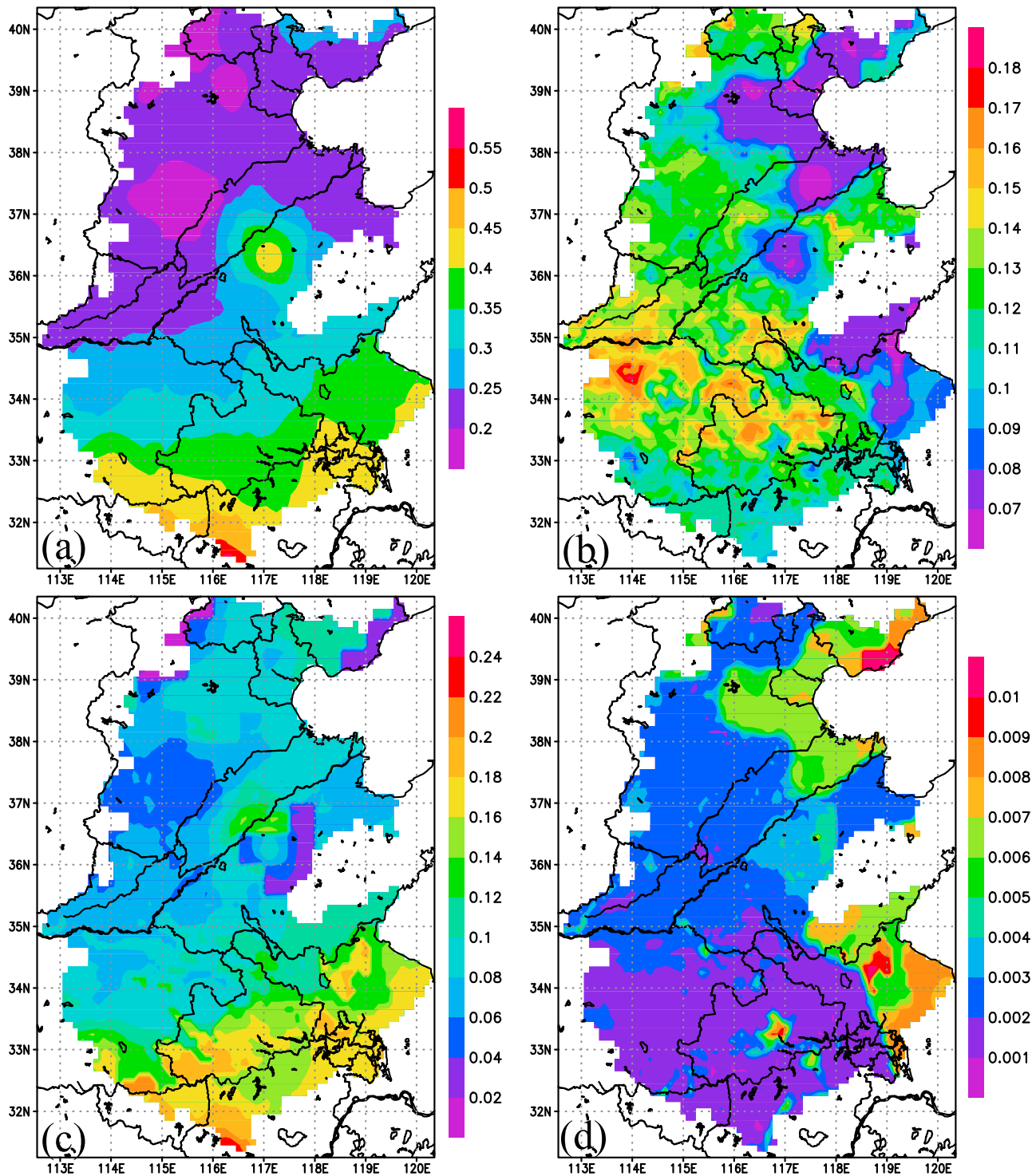


Figure 6. The climatology of the climate scenario 6 (+2°C and 15% precipitation anomaly) minus the normal observed climatology of 3H over China: (a) the precipitation difference, (b) ET difference, (c) runoff difference (units: mm/day), and (d) volumetric soil moisture difference of the top layer (units: m^3/m^3).

reduction can be attributed to increased evapotranspiration, which will cause reduction of the runoff according to the surface water budget. The soil moisture still shows a small increase in the north and a decrease in the southern parts of the 3H region with the boundary around 35°N. The obvious decreasing soil moisture occurs in Jiangsu and Bohai Bay

and the decreasing magnitude is enhanced in contrast with 2°C warming.

[30] Surface water changes under the climate change of scenario 11, with 5°C warming and +15% precipitation variation, show increasing fluxes (Figure 9). The ET (Figure 9b) change presents the largest increase to the south of 34°N with

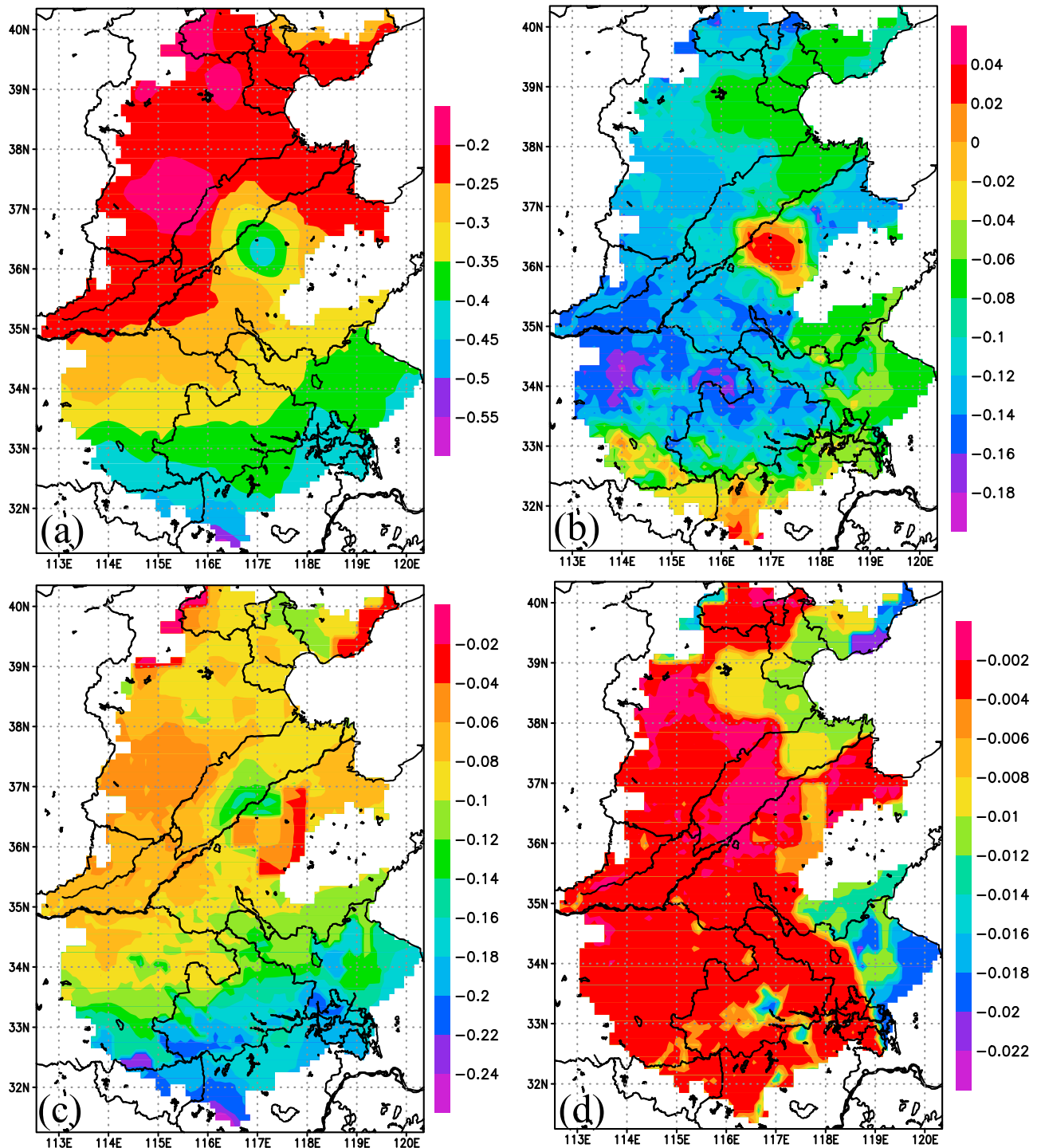


Figure 7. The climatology of the climate scenario 7 (+2°C and -15% precipitation anomaly) minus the normal observed climatology of 3H over China: (a) the precipitation difference, (b) ET difference, (c) runoff difference (units: mm/day), and (d) volumetric soil moisture difference of the top layer (units: m^3/m^3).

values more than 0.2 mm/day, and is generally larger than that of climate scenario 6 (Figure 6b). The southern end of the 3H region is unique, showing a greater increase in ET in contrast with the values below 0.12 mm/day under 2°C warming. The effect of higher temperature rise on ET is again shown to mainly occur in the southern end of the 3H region. The runoff (Figure 9c) increases across the 3H region and the largest

increment is located to the south of 34°N. The northwestern part of the region, between 34 and 39°N, shows low runoff increase, below 0.08 mm/day. The soil moisture increases more in the north than in the south and the obvious increases are located to the north of 36°N. This is because of less precipitation being allocated to the enhanced ET and

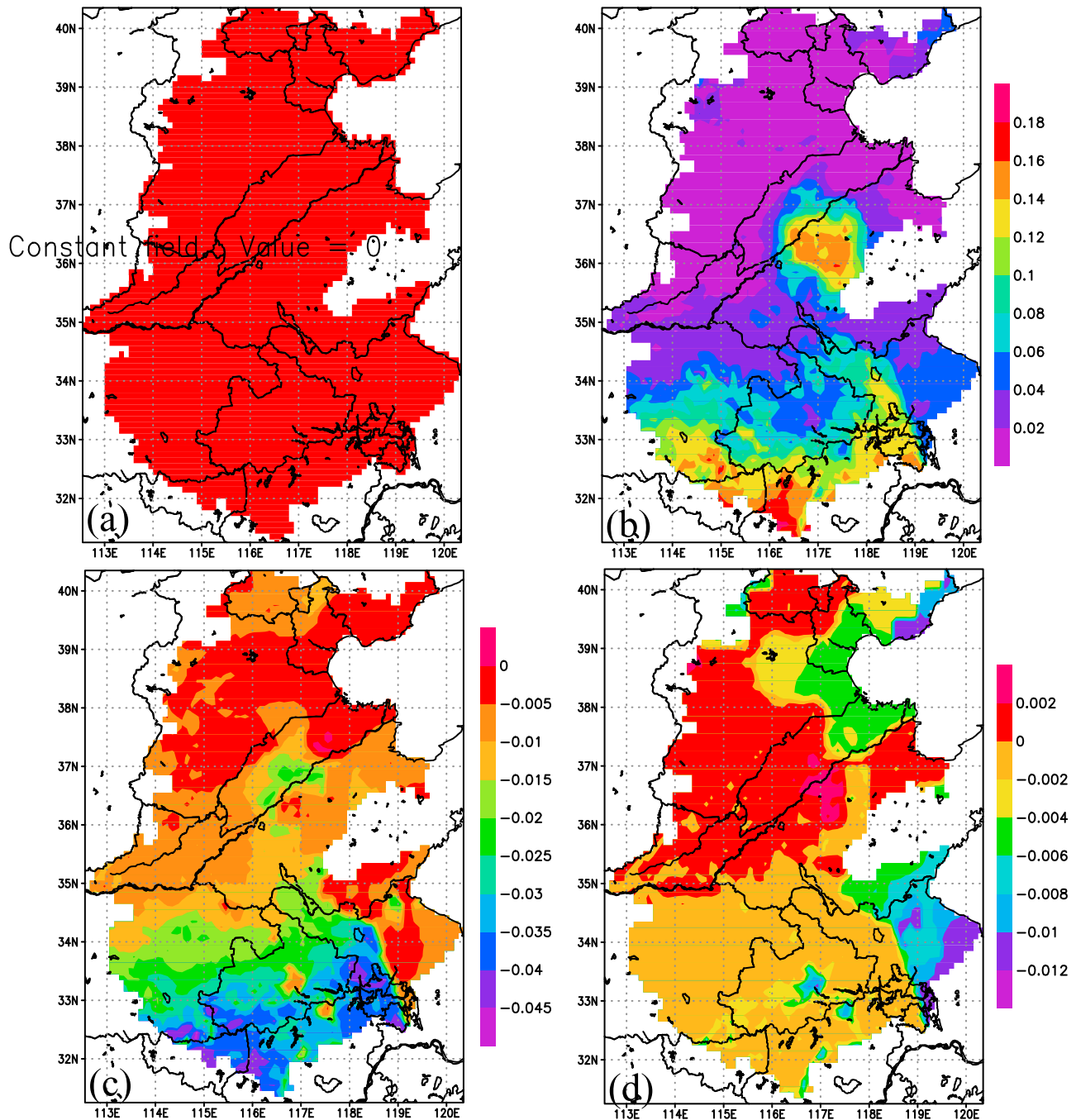


Figure 8. The climatology of the climate scenario 10 (+5°C anomaly) minus the normal observed climatology of 3H over China: (a) the precipitation difference, (b) ET difference, (c) runoff difference (units: mm/day), and (d) volumetric soil moisture difference of the top layer (units: m^3/m^3).

runoff under scenario 11 in the northern 3H in contrast with the southern 3H.

[31] In comparison, the climate change scenario of +5°C and -15% precipitation (scenario 12), show pronounced decreases (Figure 10). The ET change (Figure 10b) shows a decreasing pattern across the 3H region, except for Taishan Mountain and the southern end of the 3H region. Compared to the ET change in scenario 7 of +2°C and -15% precipitation (Figure 7b), ET is similar in most areas in the 3H region except for Taishan Mountain and the southern end, where

relatively adequate water for surface evaporation leads to higher ET under a 5°C temperature rise. Runoff data shows decreasing patterns over the 3H region, with a remarkable decrease occurring south of 34°N. The runoff decreases are similar over the 3H region in contrast with scenario 7 (Figure 7c), which reveals that the 5°C warming has nearly the same effect as a 2°C rise. The soil moisture decreased in Jiangsu province, which is also similar to the results of scenario 7. In contrast to scenario 7, there is a greater decrease in the south.

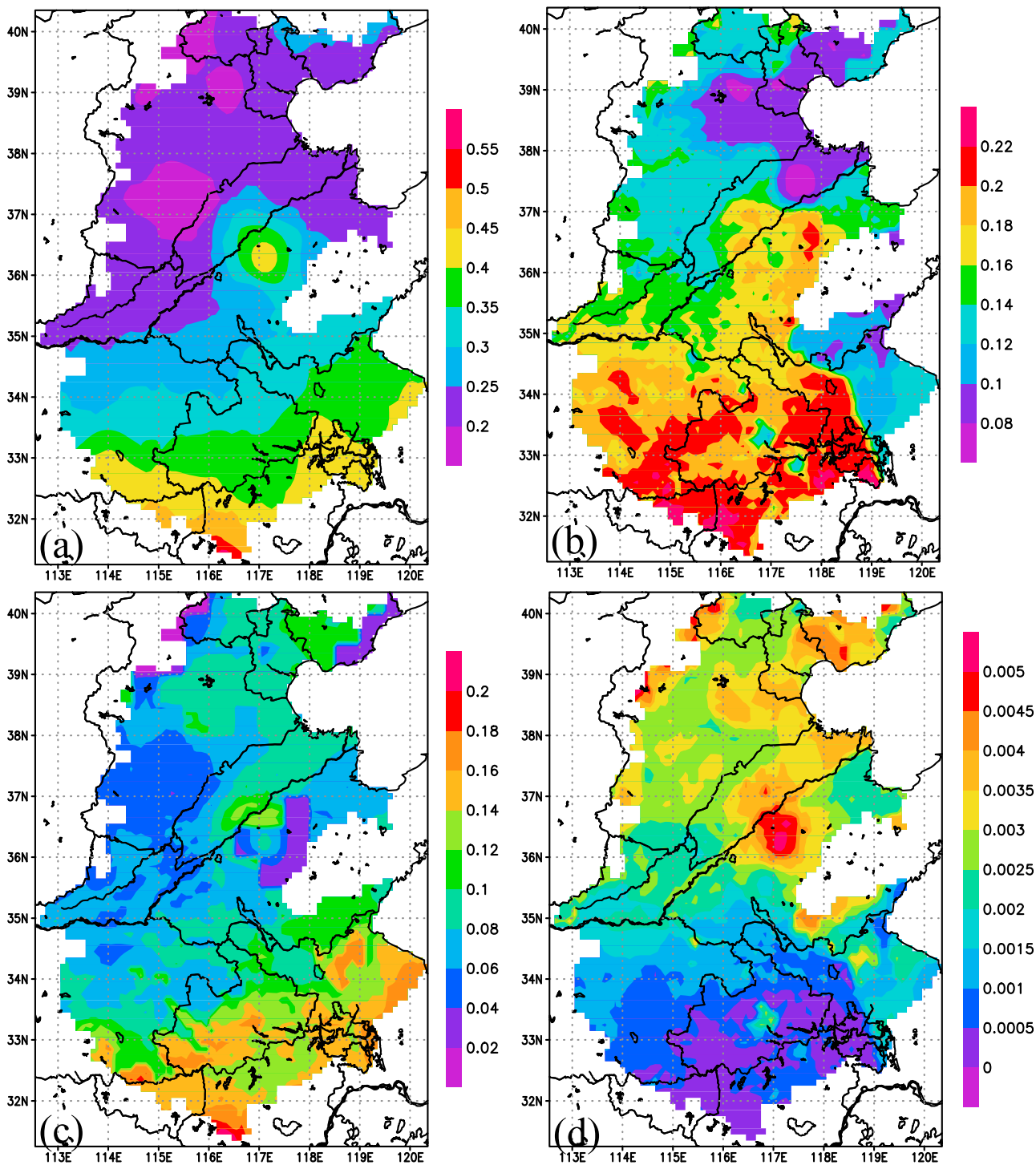


Figure 9. The climatology of the climate scenario 11 (+5°C and 15% precipitation anomaly) minus the normal observed climatology of 3H over China: (a) the precipitation difference, (b) ET difference, (c) runoff difference (units: mm/day), and (d) volumetric soil moisture difference of the top layer (units: m³/m³).

3.3. Simulations Averaged Over the 3H Region

[32] We now examine precipitation, ET, runoff and soil moisture averaged across the 3H region (Table 3). For soil moisture, we focus on results from the top layer, as it is the most sensitive to temperature and precipitation change, and is where most crops are. Patterns in total column soil moisture

are comparable, except in the southern 3H, along 33°N and to west of 119°E (Table 3).

[33] Results demonstrate the dominating effect of precipitation on ET, in that evaporation decreases with less precipitation, even when temperature was increased from +2°C to +5°C. The changes in ET were nonlinearly related to the changes in precipitation, being more sensitive to a

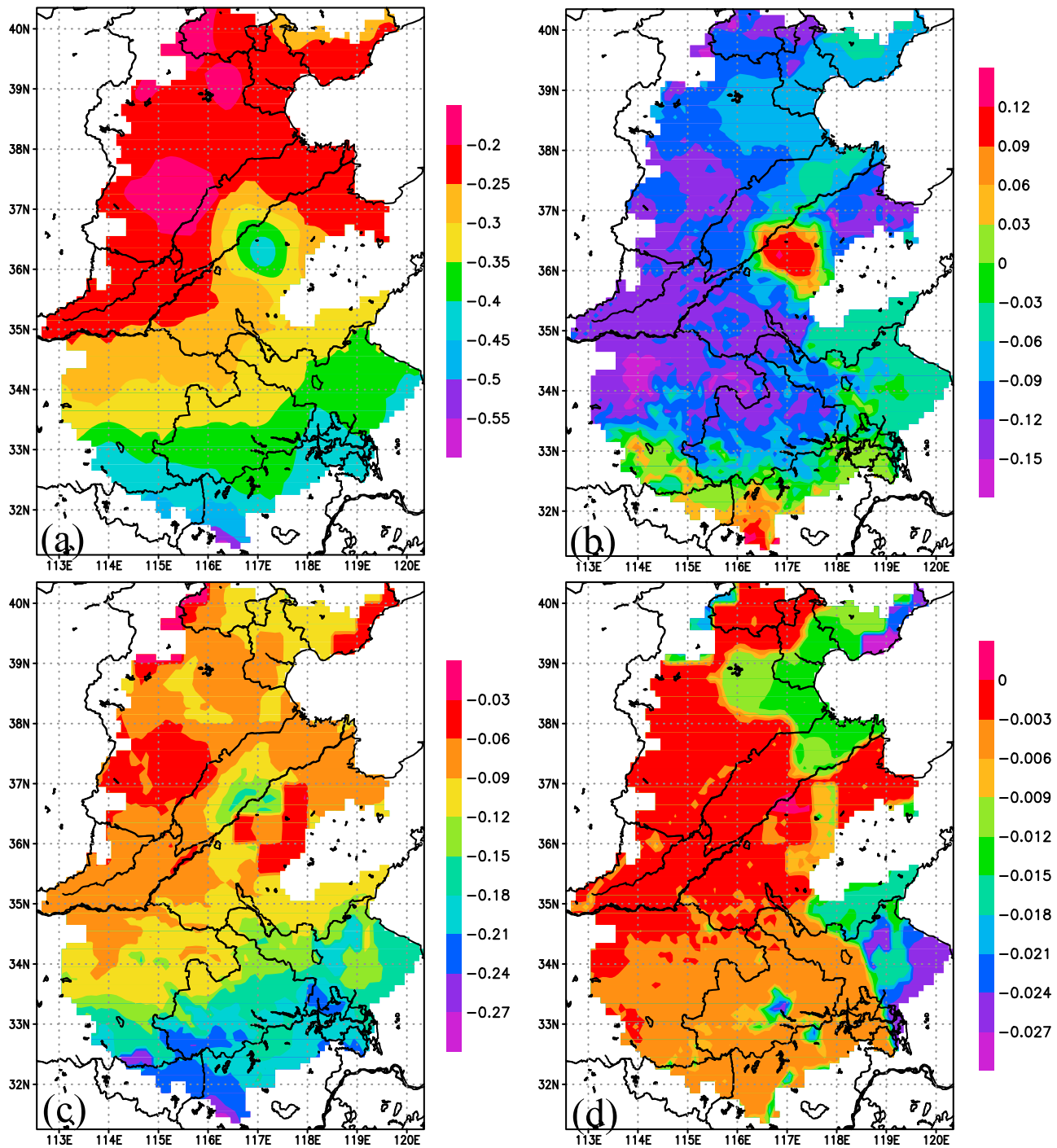


Figure 10. The climatology of the climate scenario 12 (+5°C and –15% precipitation anomaly) minus the normal observed climatology of 3H over China: (a) the precipitation difference, (b) ET difference, (c) runoff difference (units: mm/day), and (d) volumetric soil moisture difference of the top layer (units: m^3/m^3).

30% decline than a 30% increase. Similarly, soil moisture of the top layer and total column appeared to be non-linearly related to changes in precipitation, with the greatest sensitivity being related to a decline in precipitation. Runoff, however, was approximately linearly related to precipitation. Compared to scenarios of 15% change in

precipitation, the 30% change in precipitation has a similar impact on ET change in both upward and downward trends, although there is a higher value of ET change from 30% change of precipitation. As for the difference between scenarios of $\pm 30\%$ and $\pm 15\%$ change of precipitation, ET is more sensitive to a 30% decline in precipitation than a 30%

Table 3. The Area-Averaged Surface Hydrological Variation in the 3H Region as Follows: Normal, +2°C and +5°C for Temperature; ±15% and ±30% Change for Precipitation^a

Variable	Normal_P	15%P	-15%P	30%P	-30%P
Pre (mm/day)					
Normal_T	1.95	1.95+0.29	1.95-0.29	1.95+0.58	1.95-0.58
+2°C	1.95	1.95+0.29	1.95-0.29		
+5°C	0	1.95+0.29	1.95-0.29	1.95+0.58	1.95-0.58
ET (mm/day)					
Normal_T	1.26	1.26+0.09	1.26-0.11	1.26+0.16	1.26-0.25
+2°C	1.26+0.02	1.26+0.12	1.26-0.10		
+5°C	1.26+0.05	1.26+0.15	1.26-0.08	1.26+0.24	1.26-0.23
Rof (mm/day)					
Normal_T	0.46	0.46+0.11	0.46-0.10	0.46+0.22	0.46-0.19
+2°C	0.46-0.005	0.46+0.11	0.46-0.10		
+5°C	0.46-0.01	0.46+0.09	0.46-0.11	0.46+0.20	0.46-0.20
Sm (m ³ /m ³)					
Normal_T	0.25	0.25+0.00389	0.25-0.00458	0.25+0.00727	0.25-0.01013
+2°C	0.25-0.00054	0.25+0.00332	0.25-0.00508		
+5°C	0.25-0.0017	0.25+0.0021	0.25-0.00617	0.25+0.00541	0.25-0.0116
St (m ³ /m ³)					
Normal_T	0.27	0.27+0.02348	0.27-0.02787	0.27+0.04091	0.27-0.05876
+2°C	0.27-0.00568	0.27+0.01836	0.27-0.03304		
+5°C	0.27-0.01422	0.27+0.01030	0.27-0.04152	0.27+0.03004	0.27-0.07033

^aPre and P for precipitation, T for temperature, ET for evapotranspiration, Rof means runoff, Sm means the first-layer soil moisture, St means the total soil moisture, normal means no changes of temperature or precipitation, the symbol % shows the extent of change.

increase. ET decreases by more than double from -15% to -30%, in contrast to the difference between a 15% and 30% change, which shows there is not a linear sensitivity of ET to rainfall.

[34] The soil layer in most areas of the 3H exists in a relatively dry state, with the surface water surplus equivalent to the precipitation minus runoff and ET, which is very small and accounts for about 11.5% of precipitation [*Chinese Academy of Sciences*, 2007]. If precipitation increases, the surface hydrology will be enhanced, and then will rise to a stable state of saturation. This is especially true for the surface water which flows in the form of runoff. However, if the precipitation declines substantially, e.g., the -30% of this study, the surface hydrology of the soil moisture will be more sensitive to a decrease in rainfall than an equivalent increase due to the persistent drought damage with the memory capacity of the soil. This potential drought damage may cause ecological disasters in the 3H region.

[35] To investigate the sensitivity or elasticity of runoff change to climatic change, the ratios of runoff difference to precipitation difference in the four scenarios (+2°C with ±15% precipitation and +5°C with ±15% precipitation) were analyzed (Figure 11). For the winter wheat and summer maize in 3H, the growing season is mainly from April to September [*Chinese Academy of Sciences*, 2007]. Consequently, the ratios in the growing season are presented, noting that their spatial change is similar to the annual average (not shown). The precipitation decrease with 2° or 5° rise has larger impact on runoff (by comparing Figures 11b and 11a and Figures 11d and 11c). The absolute value of the reduced runoff with -15% precipitation is larger than the increased value with +15% change, thus the ratio is greater in the -15% change of precipitation. For the +15% precipitation change, the runoff increase with 5° rise is smaller than 2° rise due to the larger ET (Figures 6b and 9b). For the -15% precipitation change, the

runoff decrease with 5° rise is higher than 2° rise (which makes the ratio of Figure 11d higher than that of Figure 11b).

4. Conclusions and Discussion

[36] This study uses the VIC model to explore the current and future hydrological changes in the 3H region of China, where changes are represented by surface ET, runoff and soil moisture. Rainfall is the dominant control on the hydrology, with temperature primarily inducing changes in ET. There is a strong contrast in the magnitude of this response from the north to south of the 3H region. Marked variations of the soil moisture occur in the Jiangsu province of East China. The reason for this is complicated and may be related to the soil texture of sand silt [*Xie et al.*, 2004; *Zhang et al.*, 2004] and its close proximity to the sea [*Dan et al.*, 2005]. In reality, it should be noticed that the future dry-warm condition (e.g., 2°C rise and minus 15% precipitation change) may lead to a decrease of runoff and soil moisture over 3H. Groundwater will decrease with a decline in precipitation and water recharge.

[37] *Wang et al.* [2011] projects the future runoff change across China in 2021–2050, under A2 and B2 scenarios with about 2° warming and slightly increased precipitation percentage (2.1–8.7%). This runoff change is the opposite in the 3H (cf. middle and lower figures of Figure 8 by Wang et al.). This is despite the same upward trend of climate change, which shows generally increased runoff in A2 and decline in B2 for both annual mean and flood seasonal average from June to September. However, our scenario 6 (+2°C and 15% precipitation) shows increased runoff for annual mean (Figure 6c) and growth seasonal average (figures not shown), and only decline (Figure 7c) in scenario of 7, with a -15% precipitation change. This discrepancy of runoff change can be attributed to the large uncertainty in future climate change scenarios, and to different spatial scales,

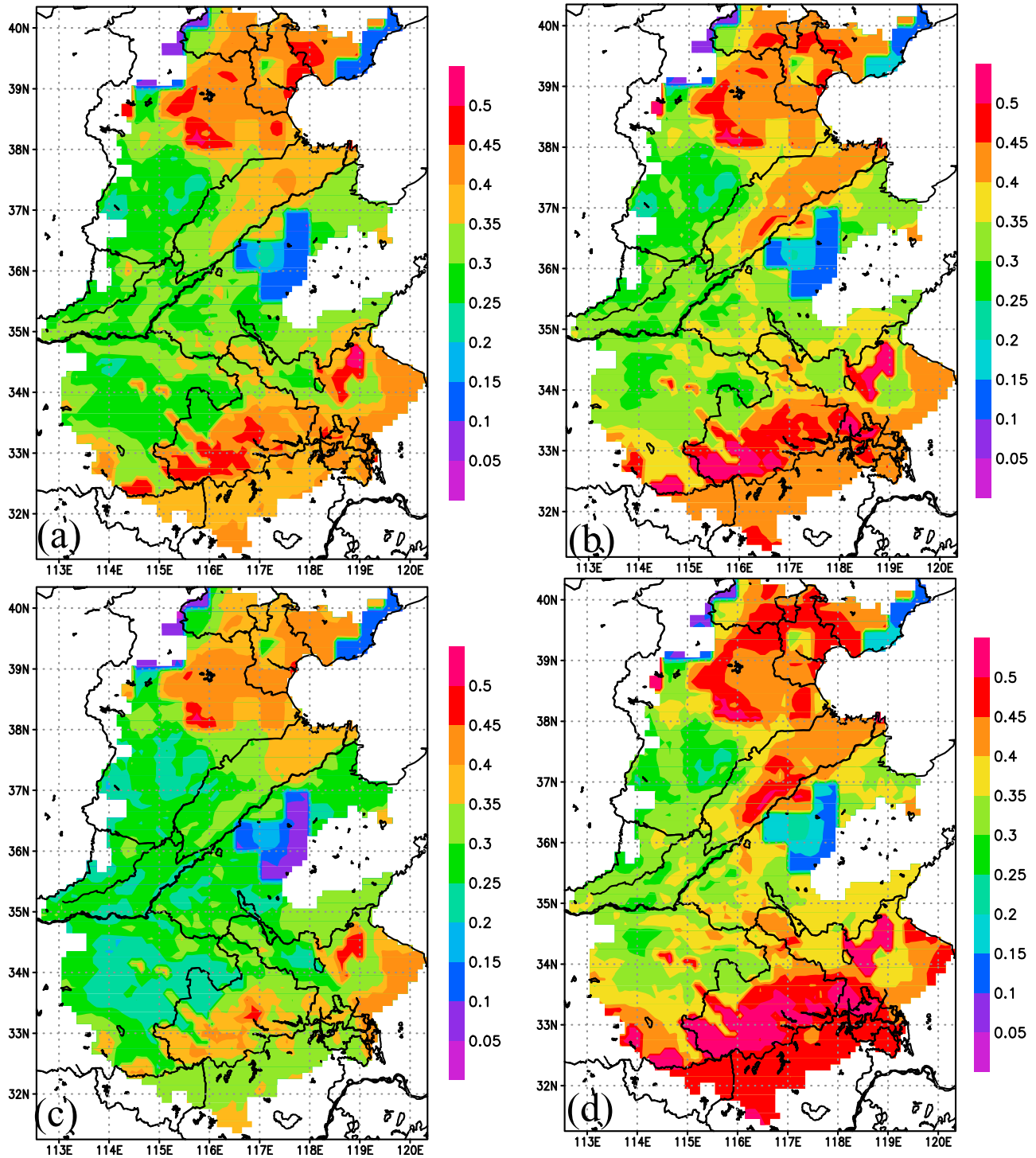


Figure 11. The ratio of runoff difference to precipitation difference for climate scenarios minus the normal observed climatology of 3H over China in growing season: (a) scenario 6 with $+2^{\circ}\text{C}$ and 15% precipitation anomaly, (b) scenario 7 with $+2^{\circ}\text{C}$ and -15% precipitation anomaly, (c) scenario 11 with $+5^{\circ}\text{C}$ and 15% precipitation anomaly, and (d) scenario 12 with $+5^{\circ}\text{C}$ and -15% precipitation anomaly (units: dimensionless).

which reflects the complicated regionality of runoff in 3H and the necessity of finer scaled simulations using different combinations of climate change to assess the risk of future runoff change.

[38] The $+5^{\circ}\text{C}$ of temperature and $\pm 30\%$ precipitation change bounds future climate change in China's 3H region due to global warming. In past decades in the 3H, temperature rise and precipitation decrease have occurred. Scenario 7 ($+2^{\circ}\text{C}$ and -15% precipitation) may be closer to a reality

in future decades based on climate projections of northern China. From the impact of different scenarios on surface water, we see that the effect of precipitation is more significant than temperature change. For instance, the increase of 15% precipitation can offset the decreasing phenomenon due to 2°C warming and lead to the rise of runoff and soil moisture over the 3H. The results of +5°C is similar to that of +2°C in spatial pattern, where only the variation range is different. The 15% and 30% change of precipitation also show a similar spatial pattern with changing magnitudes.

[39] Due to the precipitation decrease with a warming trend, the decline in runoff and increased ET will cause drought over the 3H, especially in spring and autumn, to the detriment of agriculture. Because of this, it will be critical to utilize water sources as efficiently as possible over the 3H. Based on the results here, adaptation strategies can be identified. The spatial distributions of the predicted changes are regarded as the scientific basis for different counties to adopt the relevant measures of water management adaptation to climate change, to ensure future food and water security based on maintaining water availability.

[40] This study suggests adaptation to future climate change that focuses on the comprehensive usage of rainfall and surface water, so that the over-extraction of groundwater can be minimized. The projected changes are large enough to be significant to local water resources, such as the decreasing runoff of 0.1 mm/day occupying 21.7% of the 0.46 mm/day runoff across 3H under the scenarios of +2°C and -15%, especially in representative counties (figures not shown), with variation in runoff ranging from 25 to 30%. The likely impact of climate change on crops in the scenarios has been well-summarized by Liu *et al.* [2010], which accounts for the negative effect of temperature rise without considering CO₂ fertilization due to a shorter optimal growth period under higher air temperatures. An increase of 15% or 30% precipitation will offset the negative impact of temperature to a degree. The impact on groundwater under the broad climate scenarios was explored by Xie *et al.* [2009], by using the ET and precipitation derived from VIC to drive a statistical model, RTFN. Their study showed that the fluctuation of annual mean water table depth (WTD) over 3H varies from -81 to 96 mm, with a larger change in WTD in the south of 3H than in the north. The effect of precipitation change on WTD was more obvious than that of a rise in the temperature.

[41] This analysis shows that the 3H region is indeed susceptible to changes in precipitation and temperature, with negative implications for water resources. Future work needs to be done on water resource management for the comprehensive rational usage of rainfall, surface water and groundwater as critical resources. Based on climate change predictions, the surface water resources (river, reservoir, pool and canal), and shallow groundwater can be mainly used before the flood season. Recharge of groundwater should be implemented during the flood season. For the regions with markedly increasing ET, it is important to decrease the area of water consuming crops, and increase drought tolerant crops. The development of agricultural techniques, e.g., straw stalk cover, can also be adopted to reduce the ET of field soil moisture capacity. For groundwater, some regions can be established as moderate areas where controlled extraction is allowed, whereas other regions must be regulated as strictly prohibited extraction areas. Finally, through

the overall management and deployment of different water resources, the extraction of deep groundwater can decrease and be substituted gradually.

[42] **Acknowledgments.** This study was supported by the GEF/World Bank “Mainstreaming Adaptation to Climate Change into Water Resources Management and Rural Development” project implemented by the State Office for Comprehensive Agricultural Development (SOCAD) of China, the Knowledge Innovation Program of the Chinese Academy of Sciences (KZCX2-EW-QN208), the project of National Natural Science Foundation of China (grant 40730106), the National Basic Research Program of China (grant 2010CB428502, 2011CB952003), and the R&D Special Fund for Public Welfare Industry (meteorology) by the Ministry of Finance and the Ministry of Science and Technology (GYHY200906020, GYHY201006014). Thanks are also given to Dennis Lettenmaier and Alexandra Richey for their language revisions on this paper.

References

- Arnell, N. W. (2003), Relative effects of multi-decadal climatic variability and changes in the mean and variability of climate due to global warming: Future streamflows in Britain, *J. Hydrol.*, 270, 195–213, doi:10.1016/S0022-1694(02)00288-3.
- Arnell, N. W. (2011), Uncertainty in the relationship between climate forcing and hydrological response in UK catchments, *Hydrol. Earth Syst. Sci.*, 15, 897–912, doi:10.5194/hess-15-897-2011.
- Cai, X. M. (2008), Water stress, water transfer and social equity in northern China—Implications for policy reforms, *J. Environ. Manage.*, 87, 14–25, doi:10.1016/j.jenvman.2006.12.046.
- Cherkauer, K. A., L. C. Bowling, and D. P. Lettenmaier (2003), Variable Infiltration Capacity (VIC) cold land process model updates, *Global Planet. Change*, 38, 151–159, doi:10.1016/S0921-8181(03)00025-0.
- Chinese Academy of Sciences (2007), Science-based understanding for GEF “Mainstreaming Adaptation to Climate Change into Water Resources Management and Rural Development” project implementation plan, report, pp. 156, Beijing.
- Dan, L., J. Ji, and P. Zhang (2005), The soil moisture of China in a high resolution climate-vegetation model, *Adv. Atmos. Sci.*, 22, 720–729, doi:10.1007/BF02918715.
- Diaz-Nieto, J., and R. L. Wilby (2005), A comparison of statistical downscaling and climate change factor methods: Impacts on low flows in the river Thames, United Kingdom, *Clim. Change*, 69, 245–268, doi:10.1007/s10584-005-1157-6.
- Ding, Y., and X. S. Dai (1994), Temperature variation in China during the last 100 years (in Chinese), *Meteorol. Monogr.*, 20, 19–26.
- Elsner, M. M., L. Cuo, N. Voisin, J. S. Deems, A. F. Hamlet, J. A. Vano, K. E. B. Mickelson, S. Y. Lee, and D. P. Lettenmaier (2010), Implications of 21st century climate change for the hydrology of Washington state, *Clim. Change*, 102, 225–260, doi:10.1007/s10584-010-9855-0.
- Food and Agriculture Organization (1998), *Digital Soil Map of the World and Derived Soil Properties* [CD-ROM], FAO Land and Water Div., Rome.
- Gong, G. (1985), The primary discussion on the range of Huang-Huai-Hai Plain (in Chinese), in *The Management and Development of Huang-Huai-Hai Plain*, edited by Z. Dakang, pp. 1–8, Science, Beijing.
- Hamlet, A. F., and D. P. Lettenmaier (1999), Effects of climate change on hydrology and water resources of the Columbia River basin, *J. Am. Water Resour. Assoc.*, 35, 1597–1623, doi:10.1111/j.1752-1688.1999.tb04240.x.
- Kirono, D., K. Hennessy, F. Mpelasoka, and D. Kent (2011), Approaches for generating climate change scenarios for use in drought projections: A review, *Tech. Rep. 34*, pp. 34, Cent. for Aust. Weather and Clim. Res., Melbourne, Vic., Australia.
- Liang, X., D. P. Lettenmaier, E. F. Wood, and S. J. Burges (1994), A simple hydrologically based model of land surface water and energy fluxes for GSMS, *J. Geophys. Res.*, 99(D7), 14,415–14,428, doi:10.1029/94JD00483.
- Liang, X., E. F. Wood, and D. P. Lettenmaier (1996), Surface soil moisture parameterization of the VIC-2L model: Evaluation and modifications, *Global Planet. Change*, 13, 195–206, doi:10.1016/0921-8181(95)00046-1.
- Liu, S. X., X. G. Mo, Z. H. Lin, Y. Q. Xu, J. J. Ji, G. Wen, and J. Richey (2010), Crop yield responses to climate change in the Huang-Huai-Hai Plain of China, *Agric. Water Manage.*, 97, 1195–1209, doi:10.1016/j.agwat.2010.03.001.
- Minville, M., F. Brissette, and R. Leconte (2008), Uncertainty of the impact of climate change on the hydrology of a nordic watershed, *J. Hydrol.*, 358, 70–83, doi:10.1016/j.jhydrol.2008.05.033.
- Mo, X. G., Z. H. Lin, and S. X. Liu (2006), Spatial-temporal evolution and driving forces of winter wheat productivity in the Huang-Huai-Hai region (in Chinese), *J. Nat. Resour.*, 21, 449–457.

- Nijssen, B., G. M. O'Donnell, A. F. Hamlet, and D. P. Lettenmaier (2001a), Hydrologic vulnerability of global rivers to climate change, *Clim. Change*, *50*, 143–175, doi:10.1023/A:1010616428763.
- Nijssen, B., G. M. O'Donnell, D. P. Lettenmaier, D. Lohmann, and E. F. Wood (2001b), Predicting the discharge of global rivers, *J. Clim.*, *14*, 3307–3323, doi:10.1175/1520-0442(2001)014<3307:PTDOGR>2.0.CO;2.
- Nijssen, B., R. Schnur, and D. P. Lettenmaier (2001c), Global retrospective estimation of soil moisture using the Variable Infiltration Capacity land surface model, 1980–1993, *J. Clim.*, *14*, 1790–1808, doi:10.1175/1520-0442(2001)014<1790:GREOSM>2.0.CO;2.
- Prudhomme, C., R. L. Wilby, S. Crooks, A. L. Kay, and N. S. Reynard (2010), Scenario-neutral approach to climate change impact studies: Application to flood risk, *J. Hydrol.*, *390*, 198–209, doi:10.1016/j.jhydrol.2010.06.043.
- Qin, D. H., Y. Y. Chen, and X. Y. Li (Eds.) (2005), *Climate and Environment Changes in China (I): Climate and Environment Changes in China and Their Projections*, pp. 562, Science, Beijing.
- Ren, G. Y., et al. (2005), Climate changes of China's mainland over the past half century (in Chinese), *Acta Meteorol. Sin.*, *63*, 942–956.
- Song, X. S., P. J. Shi, and R. Jin (2005), Analysis on the contradiction between supply and demand of water resources in China owing to uneven regional distribution (in Chinese), *Arid Zone Res.*, *22*, 162–166.
- Su, F., Y. Hong, and D. P. Lettenmaier (2008), Evaluation of TRMM Multi-satellite Precipitation Analysis (TMPA) and its utility in hydrologic prediction in La Plata Basin, *J. Hydrometeorol.*, *9*, 622–640, doi:10.1175/2007JHM944.1.
- Todd, M. C., R. G. Taylor, T. Osborne, D. Kingston, N. W. Arnell, and S. N. Gosling (2010), Quantifying the impact of climate change on water resources at the basin scale on five continents a unified approach, *Hydrol. Earth Syst. Sci. Discuss.*, *7*, 7485–7519, doi:10.5194/hessd-7-7485-2010.
- Wang, G. Q., J. Y. Zhang, J. L. Jin, T. C. Pagano, R. Calow, Z. X. Bao, C. S. Liu, Y. L. Liu, and X. L. Yan (2011), Assessing water resources in China using PRECIS projections and VIC model, *Hydrol. Earth Syst. Sci. Discuss.*, *8*, 7293–7317, doi:10.5194/hessd-8-7293-2011.
- Winkler, J. A., G. S. Guentchev, T. P. Perdinan, S. Zhong, M. Liszewska, Z. Abraham, T. Niedzwiedz, and Z. Ustrnul (2011), Climate scenario development and applications for local/regional climate change impact assessments: An overview for the non-climate scientist, *Geogr. Compass*, *5*, 275–300, doi:10.1111/j.1749-8198.2011.00425.x.
- Wu, K., and Y. X. Xu (1997), Environment effects and adjustment and control countermeasures of water resource utilization in the Huang-Huai-Hai Plain (in Chinese), *Acta Geogr. Sin.*, *52*, 114–122.
- Xia, J., R. Q. Su, X. W. He, and T. Q. Huang (2008), Water resources problems in China and their countermeasures and suggestions (in Chinese), *Strategy Policy Discuss. Res.*, *23*, 117–120.
- Xie, Z. H., Q. Liu, F. Yuan, and H. W. Liang (2004), Macro-scale land hydrological model based on 50 km × 50 km grids system (in Chinese), *J. Hydraul. Eng.*, *5*, 76–82.
- Xie, Z. H., F. Yuan, Q. Y. Duan, J. Zheng, M. L. Liang, and F. Chen (2007), Regional parameter estimation of the VIC land surface model: Methodology and application to river basins in China, *J. Hydrometeorol.*, *8*, 447–468, doi:10.1175/JHM568.1.
- Xie, Z. H., M. L. Liang, X. Yuan, F. Chen, C. Z. Liu, and Z. Y. Liu (2009), The response of shallow water table depths to climate change in Huang-Huai-Hai Plain (in Chinese), *J. China Hydrol.*, *1*, 30–35.
- Xu, J. X. (1995), A comparative study on the zonal differences in river runoff and human influence in China (in Chinese), *Geogr. Res.*, *14*, 33–42.
- Ying, A. W. (2006), The investigation and evaluation of ground water (in Chinese), *J. China Hydrol.*, *26*, 63–66.
- Zhang, S. H., G. B. Peng, and M. Huang (2004), The feature extraction and data fusion of regional soil textures based on GIS techniques (in Chinese), *Clim. and Environ. Res.*, *9*, 66–79.
- Zhou, C. C., and Q. T. Zhang (2004), The connotations of water resources crisis and the analysis of Huang-Huai-Hai Plain (in Chinese), *Territ. Nat. Resour. Study*, *1*, 79–80.